



Magnetic Point Dipole versus Finite-size Circular Loop Models in Coaxial and Coplanar Two Coil Arrays in Induction Tools.

Paulo Roberto de Carvalho* - ICIBE/UFRA, CPGf/UFPA (paulo.carvalho@ufra.edu.br); Cícero Roberto Teixeira Régis - CPGf/UFPA, INCT/GP (cicero@ufpa.br) and Allen Quentin Howard, Jr. - CPGf/UFPA, INCT/GP (terragraf@gmail.com)

Copyright 2011, SBGf - Sociedade Brasileira de Geofísica

This paper was prepared for presentation during the 12th International Congress of the Brazilian Geophysical Society held in Rio de Janeiro, Brazil, August 15-18, 2011.

Contents of this paper were reviewed by the Technical Committee of the 12th International Congress of the Brazilian Geophysical Society and do not necessarily represent any position of the SBGf, its officers or members. Electronic reproduction or storage of any part of this paper for commercial purposes without the written consent of the Brazilian Geophysical Society is prohibited.

Abstract

Until about ten years ago, all commercial borehole induction devices were built up with the traditional coaxial coil arrays. The more recent tools often include the unconventional coplanar coil arrays, in order to investigate thinly laminated reservoirs and to locate axially asymmetrical anomalies like vugs and fractures. To simplify numerical modeling of conventional borehole induction responses, point dipole sources and receivers are used instead of the more accurate loop field models. However, this approximation may not be valid for a coplanar array, in which the source and sensor axes are perpendicular to both tool and borehole axes. The main interest here is to quantify the relative difference between magnetic point dipole and finite-size loop source and receiver models in both coil arrays. We examined a range of homogeneous whole-space conductivities, multiple frequencies and source-receiver distances. We show that the relative differences between these responses vary inversely with the source-receiver spacing and directly with the conductivity and frequency range applied in standard induction tools. For both coil arrays, coaxial and coplanar, the magnetic dipole mathematical model, particularly for shorter spacings and higher frequencies and conductivities, may not be adequate. In some very common cases the discrepancy in the voltage induced in the sensors may be almost 1% for the real component and 2% for the imaginary.

Introduction

None of the traditional E.M. borehole induction devices possessed azimuthal focusing properties until about 10 years ago, whereas the unconventional coplanar coil array had, by design, a strong azimuthal focus. This characteristic of coplanar coil arrays had been explored for many decades in surface electromagnetic surveys. That prompted Moran & Gianzero (1979) and Kaufman & Keller (1989) to investigate the application of this transverse EM induction array in simple geometries of the borehole environments. For a better understanding of the

coplanar responses in a borehole, the group led by Prof. Om Verma in the Federal University of Pará build laboratory models (Carvalho & Verma, 1994; Souza & Verma, 1995 and Carvalho & Verma, 1998) as well as one-dimensional numerical models (Santos, 2007 and Carvalho et al., 2010). Krigshäuser et. al, (2000) presented a multi-coil array to evaluate thinly laminated sand/shale sequences, encountered in deep-water turbidites. Basically, in such triaxial induction tools there are three source coils, one that is coaxial with the borehole axis and two that are transverse to it as shown in Fig. 1.

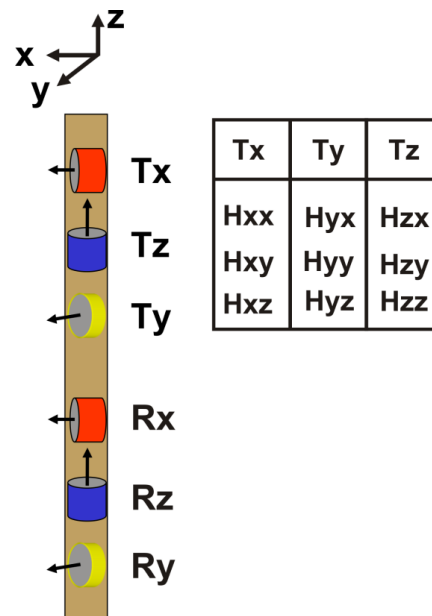


Figure 1. Triaxial induction tool and their nine magnetic field components.

Wang et. al (2003) showed that the nine magnetic field components are different only in tridimensional and/or anisotropic environments. Lu & Alumbaugh (2001) applied the six cross-coupled components to define the tool's azimuthal position into the borehole. Souza & Verma (1995) were one of the first to explore the azimuthal focusing properties of the coplanar array in the borehole investigation of asymmetrical geological situations such as vugular and fracture zones.

Two major limitations of uniaxial induction tools (coaxial arrays) are the incorrect resistivity reading in dipping beds and in anisotropic layers. Anderson et. al (2008) show some case studies where these limitations are overcome by the triaxial induction (coaxial and coplanar arrays together) measurements. More accurate resistivity leads to more accurate water saturation, which enables petrophysicists to correctly evaluate hydrocarbon reservoirs.

Following Ellis & Singer (2007), in this work we ignore the six cross-coupled components of the Fig. 1 (H_{xy} , H_{xz} , H_{yx} , H_{yz} , H_{zx} , and H_{zy}) and compare only the responses obtained from the coaxial array (H_{zz}) with the two coplanar arrays (H_{xx} and H_{yy}), inasmuch as they are the most important signals of the triaxial tool. Moreover, due to the simplicity of the infinite homogeneous medium the two coplanar components are identical in our cases.

Almost all induction computer logs approximate the loop circular antennas of the actual tools with magnetic point dipole. This approximation neglects the radial structure of the tool, specifically, the mandrel with the antenna recesses. In the literature this assumption has been accepted since the radii of the coils are small compared to the source-receiver spacing and the wavelength. However, the point dipole approximation must be carefully tested and validated for the triaxial induction tool because that approximation for the coplanar array is not at the same level as that for the coaxial array.

The experimental test tank results of Carvalho & Verma (1998) show a small difference from the theoretical predictions modeled by Howard & Chew (1992) in front of the bed interfaces. This small discrepancy is mainly caused by the point dipole approximation of the modeled antennas. The dipole assumption in the computer logs overestimate the horns in front of the bed boundaries, caused by the charge build-up at the interfaces. Anderson et al. (1990) show that the point dipole approximation enhances these horns in synthetic logs which appear smeared out on the field log due to the finite size of the loop and the presence of the borehole. The dipole in the computer model has a single intersection point with the interface while the actual coplanar loop antenna crosses the interface an extended interval. For a coaxial array Howard (1997) shows that the finite-size loop antenna with axis parallel to planar horizontal interface and the horizontal magnetic dipole (HMD) can depart by 10 to 15% when the source-sensor spacing in a coaxial array is less than four times the loop radii.

It is known that for the cases near the source, the magnetic point dipole approximation deviates from the more accurate loop field modes. To quantify this discrepancy, we show the analytical and semi-analytical solutions to the voltages induced in the receivers for coaxial and coplanar coil arrays in an infinite conductive homogeneous space.

Method

The objective here is to quantify the relative differences, in percentage, between the voltages considering the source and sensor like magnetic point dipole (Eqs. 1 and

2) and finite-size circular loop (Eqs. 3 and 4), to the coaxial and coplanar two coil arrays in a whole homogeneous space. Eqs. 5 and 6 are applied to real and imaginary components of the coaxial and coplanar voltages, respectively, to obtain the relative difference for each case.

$$v_{cx}^d = -i\omega\mu\pi a^2 \frac{m}{2\pi L^3} (1 + ikL)e^{-ikL} \quad (1)$$

$$v_{cp}^d = -i\omega\mu\pi a^2 \frac{m}{4\pi L^3} [1 + ikL + (ikL)^2]e^{-ikL} \quad (2)$$

$$v_{cx}^l = -i\omega\mu\pi I a \int_0^\infty \frac{e^{-uL}}{u} J_1^2(\lambda a) \lambda d\lambda \quad (3)$$

$$v_{cp}^l = -i\omega\mu\pi I a^2 \int_0^\infty \frac{1}{u} J_1^2(\lambda a) J_0(\lambda L) \lambda d\lambda \quad (4)$$

$$d_{cx} = \left| \frac{v_{cx}^d - v_{cx}^l}{v_{cx}^d} \right| \times 100 \quad (5)$$

$$d_{cp} = \left| \frac{v_{cp}^d - v_{cp}^l}{v_{cp}^d} \right| \times 100 \quad (6)$$

The fields vary as $e^{i\omega t}$ where $i = \sqrt{-1}$; $\omega = 2\pi f$ is the angular frequency; f the linear frequency; μ the magnetic permeability, the source-sensor loops radii are $a = 0.05\text{m}$; the magnetic dipole moment is $m = \pi a^2 I$; I the electric current; L source-sensor spacing; $k = \sqrt{-i\omega\mu\sigma}$ is the wave-number; σ the medium conductivity; $u = \sqrt{\lambda^2 - k^2}$ the wave number; J_0 and J_1 are Bessel functions of the first kind of order zero and one, respectively.

These voltages for both coil arrays are obtained by the Faraday's law applied over the sensor. Eqs. (1) and (2) are closed analytical solutions obtained with the magnetic field generated by point dipole over the point sensor. Eqs. (3) and (4) are obtained with the area integration of the magnetic field generated by a loop source over the loop sensor.

Eqs. (3) and (4) have improper integrals that need to be solved numerically. The integral of the Eq. (4) does not numerically converge on the real λ -axis. To remedy this, the path of integration is deformed in the complex λ -domain, where these integrals become convergent.

Remember that the complex apparent conductivity, measured with the induction tools, are obtained dividing the voltages in the sensors by the respective array constant (Carvalho et al., 2010). Thus, this discrepancy between point dipole and finite-size loop math models may affect the theoretical estimation of the hydrocarbons in the reservoirs through the Archie formula.

Results

We examined the relative difference (%) between the dipole and loop voltages in both coil arrays, for a range of conductivities (10^{-1} to 10^0 S/m), frequencies (10 to 100kHz) and transmitter-receiver spacings (5 to 20 times the source radius).

Figs. 2.a and 2.b show that the relative differences decrease progressively as the source-sensor distance L/a increases. The data for these figures were generated at a frequency $f = 20\text{kHz}$ and conductivity $\sigma = 1\text{S/m}$. The coaxial real component is more strongly affected than the coplanar one. However, the imaginary component has an opposite behavior. Figs. 2.c and 2.d show the differences for a spacing $L = 20a$ and conductivity $\sigma = 1\text{S/m}$, with frequency. Both coaxial components increase while in the coplanar responses the real component increases and the imaginary decreases.

Fig. 3 shows the difference increase with the conductivity, for $f = 100\text{kHz}$ and $L = 10a$. The exception is the coplanar imaginary component in Fig. 3d, although it is coherent with Fig. 2d.

We are comparing the relative difference between the magnetic fields in the center of the sensor (point dipole) and over the sensor area (finite size loop). These discrepancies will be smaller when the field in the sensor area is more uniformly distributed, which happens at greater source-sensor distances. In the typical source-sensor separations and frequencies used in standard induction tools in reservoir environments, when the spacing L is much smaller than the skin depth $\delta = \sqrt{2/(\omega\mu\sigma)}$, the differences between point and finite loop receivers increase with the conductivity as well as with the frequency.

The maps of Fig. 4 show how the frequency ($f = 10$ to 100kHz) and source-sensor spacing ($L/a = 5$ to 20) affect the relative difference (%) between dipole and loop responses with a medium conductivity $\sigma = 1\text{S/m}$. We can see again that the difference vary directly with the frequency and inversely with the spacing. The real coaxial component is more strongly affected than the coplanar one, while in the imaginary components this effect is opposite.

Fig. 5 shows similar behavior where the medium conductivity changes (10^{-1} to 10^0 S/m) together with the spacing ($L/a = 10$ to 20) at a frequency $f = 20\text{kHz}$. Fig. 6 shows the direct relationship of the conductivity (10^{-1} to 10^0 S/m) and frequency ($f = 20$ to 100kHz) with the discrepancy between dipole and loop responses. Again, the imaginary coplanar component does not follow the same pattern as the coaxial one.

Conclusions

This work gives the formulation for the point dipole and finite-size loop source and receiver to the coaxial and coplanar two coil arrays in an infinite homogeneous space. The loop solutions are slightly more complicated than that of the dipoles, particularly in the coplanar array. Our numerical results show that the dipole approximation

has a greater effect on the real coaxial component than on the coplanar one. However, the imaginary components show the opposite behavior: the effect is stronger in the coplanar component.

In general, the literature describes that the dipole approximation deviates from the more accurate loop field model to spacings smaller than ten times the source radius. We would like to note here other parameters that can affect this approximation, like the medium conductivity, frequency and, mainly, the kind of geometrical coil array. In some very common cases deviations in the voltage induced in the sensors may be almost 1% for the real component and 2% for the imaginary one.

Acknowledgments

This research work is supported by the Conselho Nacional de Desenvolvimento Científico e Tecnológico (MCT/CNPq). Paulo Carvalho thanks the Instituto Clberespacial (ICIBE/UFRA) for the research facilities.

References

- Anderson BI, Borner S, Lüling MG & Rosthal R. 1990. Response of 2-MHz LWD resistivity and wireline induction tools in dipping beds and laminated formations. In: 31st Ann. Logging Sym., Soc. Prof. Well Log. Analysts, paper A.
- Anderson BI, Barber T, Bastia R, Clauvaud JB, Coffin B, Das M, Hayden R, Klimentos T, Minh CC & Williams S. 2008. Triaxial induction – A new angle for an old measurement. Oilfield Review.
- Carvalho PR de & Verma OP. 1994. Coplanar coil system in EM induction well-logging tool: 35th Ann. Logging Sym., Soc. Prof. Well Log. Analysts, paper EE.
- Carvalho PR de & Verma OP. 1998. Induction tool with a coplanar coil system: The Log Analyst, 39, No. 6, 48-53.
- Carvalho PR de, Santos, WGS and Régis, CRT. 2010. Fundamentals of Coaxial and Coplanar Coil Arrays in Induction Tools. Brazilian Journal of Geophysics, 28(1): 19-36.
- Ellis DV & Singer JM. 2007. Well logging for earth scientists. 2nd ed. Springer. 692p.
- Howard, AQ Jr. & Chew WC. 1992. Electromagnetic borehole fields in a layered dipping-bed environment with invasion. Geophysics, 57(3): 451-465.

Howard, AQ Jr. 1997. Electromagnetic fields of loop antenna with axis parallel to planar interface. Applied Geophysics, 38: 41-56. Summer: 64-84.

Kaufman AA & Keller GV. 1989. Induction logging. Amsterdam Elsevier Publishers.

Krigshäuser B, Fanini O, Forgang S, Itskovich G, Rabinovich M, Tabarovsky L. & Yu L. 2000. A new multicomponent induction logging tool to resolve anisotropic formations: 41st Ann. Logging Sym., Soc. Prof. Well Log. Analysts, paper D.

Lu X & Alumbaugh DL. 2001. One-dimensional inversion of three-components induction logging in anisotropic media. Annual International Meeting, 71. San Antonio. Expanded Abstracts – Society of Exploration Geophysics.

Moran JH & Gianzero S. 1979. Effects of formation anisotropy on resistivity-logging measurements. Geophysics, 44 (7): 1266-1286.

Santos WG dos. 2007. Arranjos coplanar e coaxial nas sondas de perfilagem de poço: ferramentas triaxiais em reservatórios laminados. MSc. Thesis, Department of Geophysics of the Federal University of Pará, Belém, Brazil. 70 p.

Souza NPR & Verma OP. 1995. Scale-model response of fracture zones to a coplanar induction tool in a borehole: The Log Analyst, 36, No 5, 49-57.

Wang H, Barber T, Rosthal R, Tabanou J, Anderson BI & Habashy T. 2003. Fast and rigorous inversion of triaxial induction logging data to determine formation resistivity anisotropy, bed boundary position, relative dip, and azimuth angles: SEG Ann. International Meeting, p. 514-517.

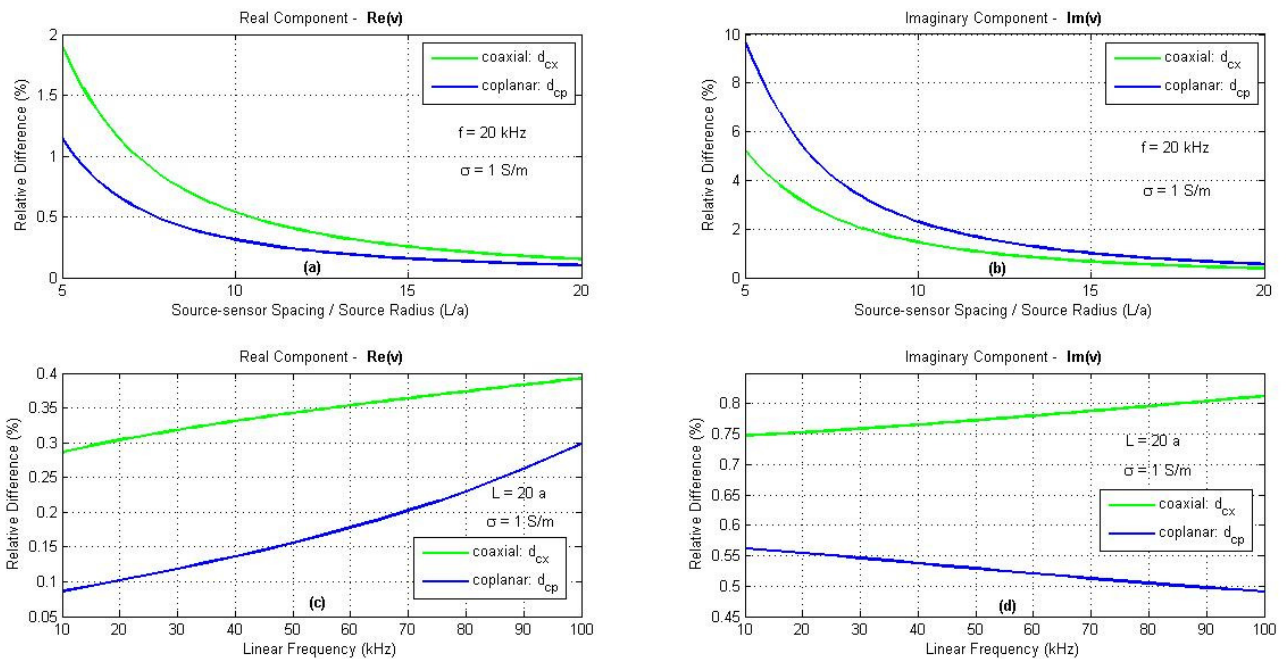


Figure 2. Relative difference between point dipole and finite-size loop models to coaxial and coplanar arrays in an infinite homogeneous space.

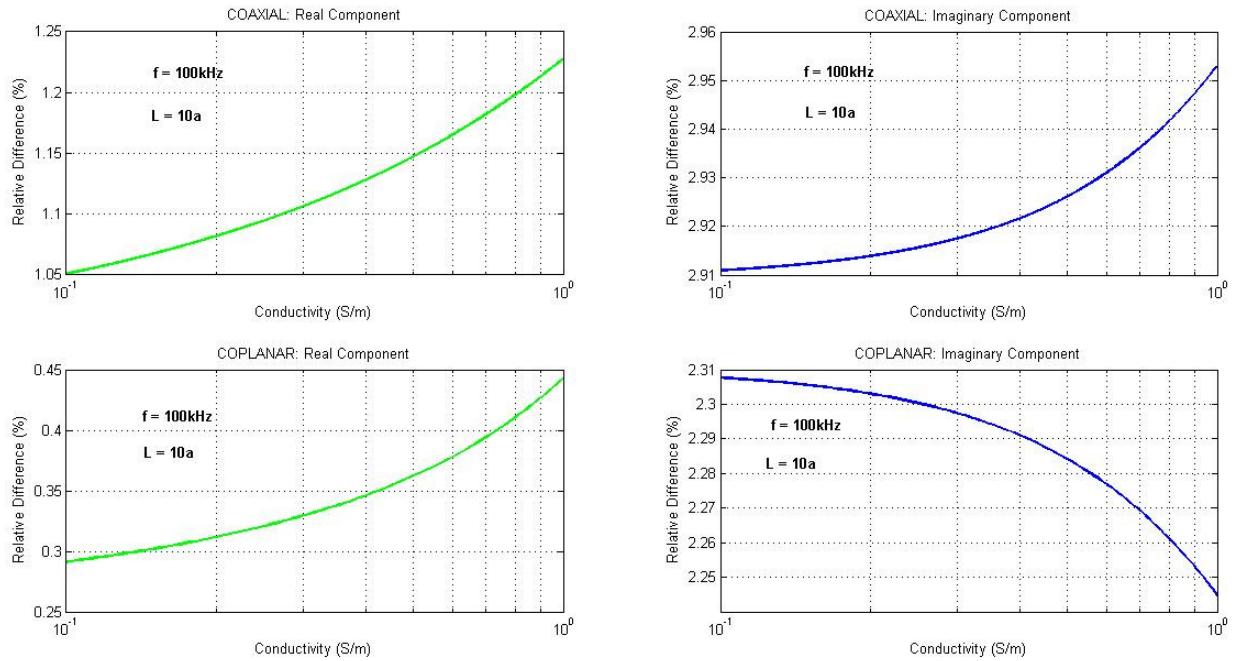


Figure 3. Relative difference between point dipole and finite-size loop models to coaxial and coplanar arrays in function of the medium conductivity.

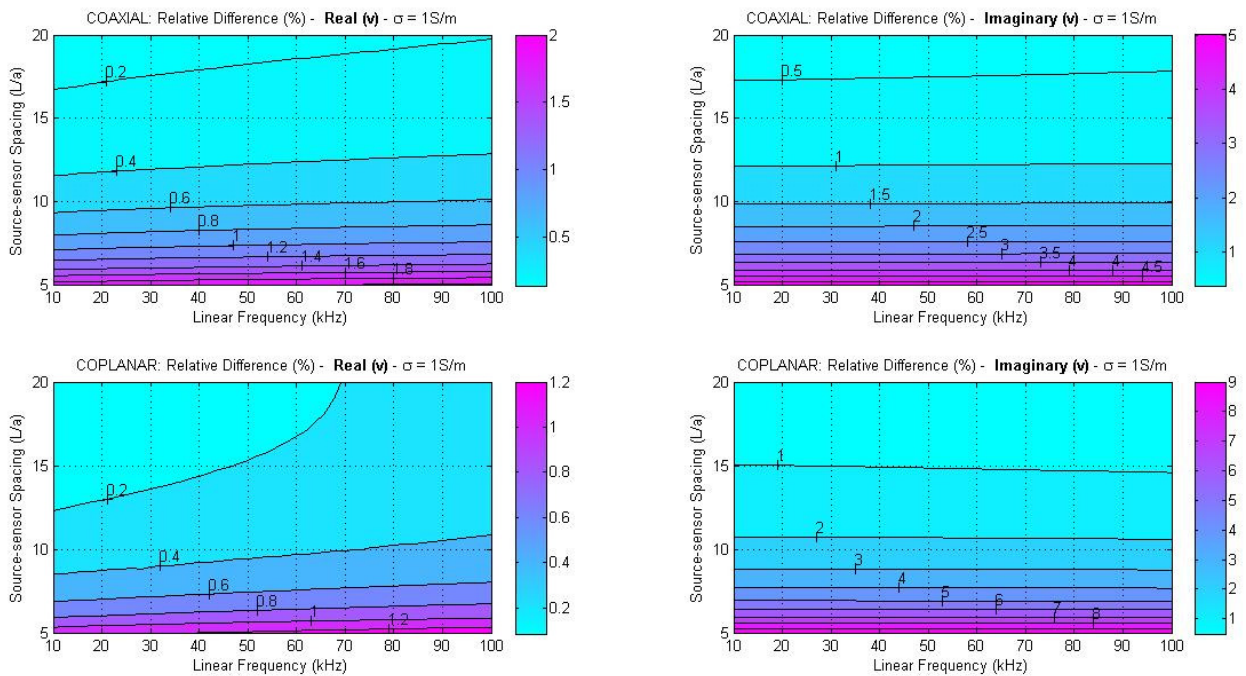


Figure 4. Relative difference between point dipole and finite-size loop models to coaxial and coplanar arrays in function of frequency and source-sensor spacing.

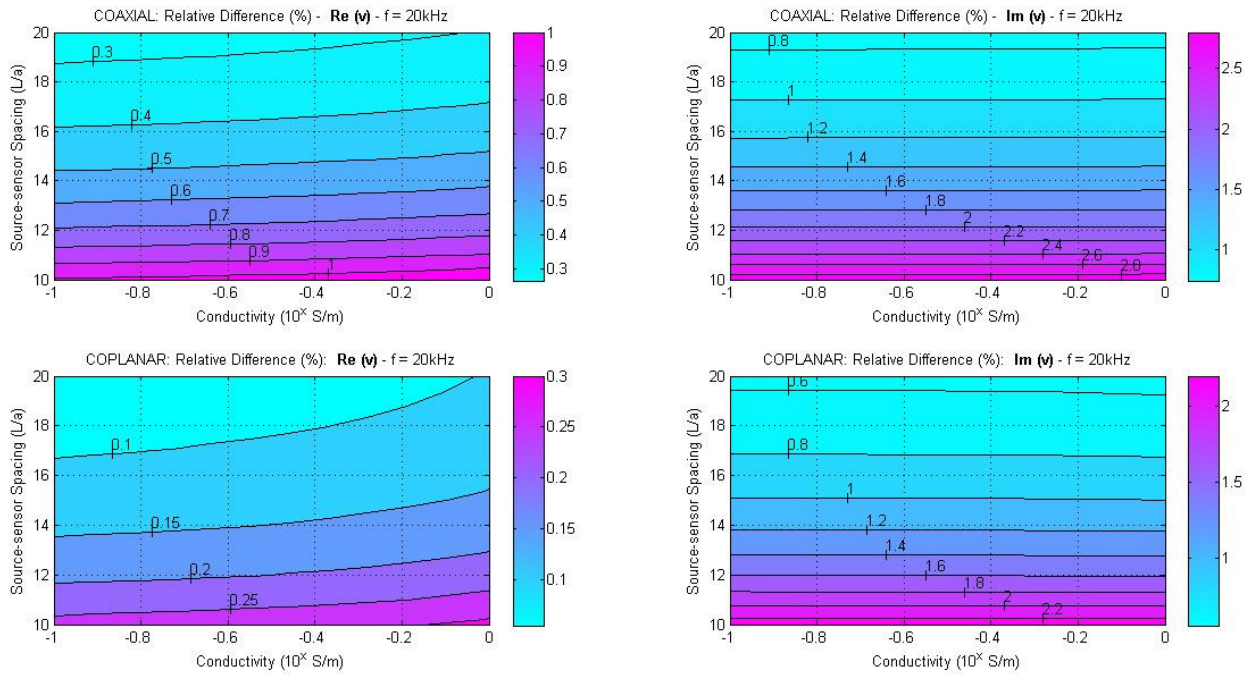


Figure 5. Relative difference between point dipole and finite-size loop models to coaxial and coplanar arrays in function of the medium conductivity and the source-sensor spacing.

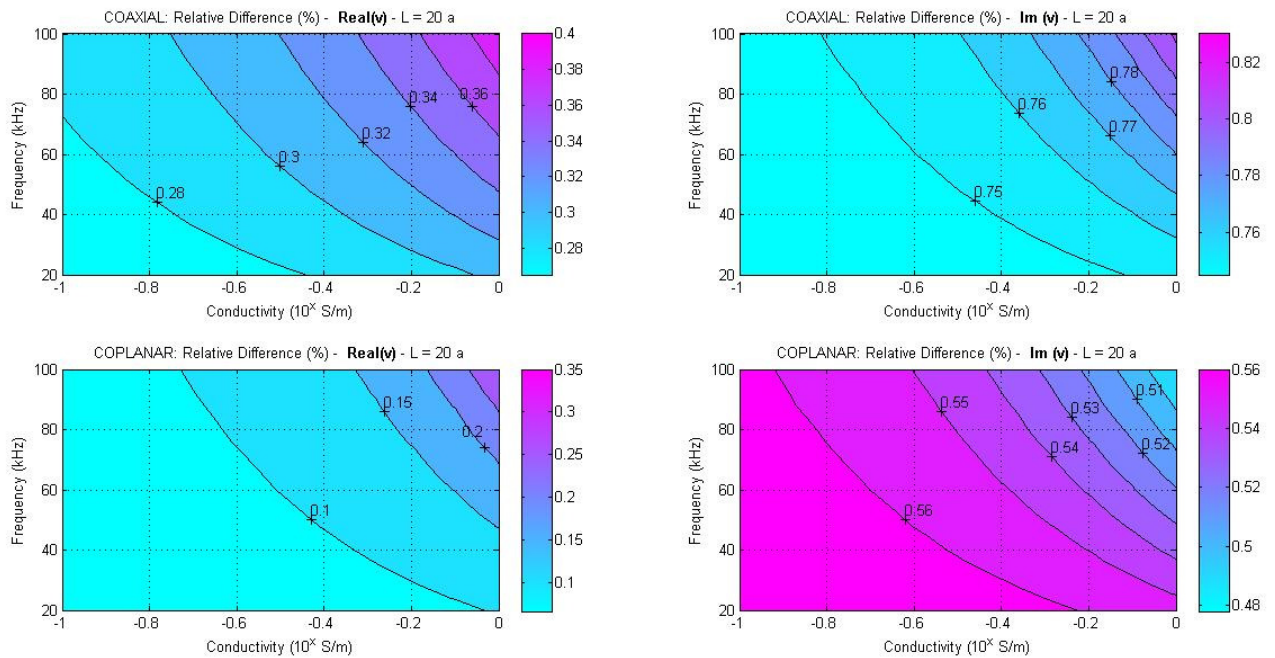


Figure 6. Relative difference between point dipole and finite-size loop models to coaxial and coplanar arrays in function of the medium conductivity and frequency.